Applied Microbiology and Biotechnology (2022) 106:5525–5538
https://doi.org/10.1007/s00253-022-12088-6

Characterization of inulolytic enzymes from the *Jerusalem artichoke*–derived *Glutamicibacter mishrai* NJAU-1

Dan Lian[1] · Shuo Zhuang[1] · Chen Shui[1] · Shicheng Zheng[1] · Yanhong Ma[2] · Zongjiu Sun[3] · Jaime R. Porras-Domínguez[4] · Ebru Toksoy Öner[5] · Mingxiang Liang[1] · Wim Van den Ende[4]

Received: 2 March 2022 / Revised: 17 July 2022 / Accepted: 20 July 2022 / Published online: 28 July 2022

Abstract

The rhizosphere context of inulin-accumulating plants, such as *Jerusalem artichoke* (*Helianthus tuberosus*), is an ideal starting basis for the discovery of inulolytic enzymes with potential for bio fructose production. We isolated a *Glutamicibacter mishrai* NJAU-1 strain from this context, showing exo-inulinase activity, releasing fructose from fructans. The growth conditions (pH 9.0; 15 °C) were adjusted, and the production of inulinase by *Glutamicibacter mishrai* NJAU-1 increased by 90% (0.32 U/mL). Intriguingly, both levan and inulin, but not fructose and sucrose, induced the production of exo-inulinase activity. Two exo-inulinase genes (*inu1* and *inu2*) were cloned and heterologously expressed in *Pichia pastoris*. While INU2 preferentially hydrolyzed longer inulins, the smallest fructan 1-kestose appeared as the preferred substrate for INU1, also efficiently degrading nystose and sucrose. Active site docking studies with GFn- and Fn-type small inulins (G is glucose, F is fructose, and n is the number of β (2–1) bound fructose moieties) revealed subtle substrate differences between INU1 and INU2. A possible explanation about substrate specificity and INU's protein structure is then suggested.

Key points

- *A Glutamicibacter mishrai strain harbored exo-inulinase activity.*
- *Fructans induced the inulolytic activity in G. mishrai while the inulolytic activity was optimized at pH 9.0 and 15 °C.*
- *Two exo-inulinases with differential substrate specificity were characterized.*

Keywords Bio fructose · Exo-inulinase · *Glutamicibacter mishrai* · Fructan · Jerusalem artichoke

Introduction

Fructans are synthesized from sucrose. Inulin (β-(2–1) glycosidic linkages) and levan (β-(2–6) glycosidic linkages) represent the two best characterized fructan classes. Plant levans and graminans (mixed linkages) occur in monocot species such as grasses and cereals. Plant inulins consist of a polydisperse mixture of shorter oligo- (degree of polymerization: DP < 10) and longer polysaccharides (DP > 10) composed of a linear chain of fructose residues terminated by one glucose residue (Van Laere and Van den Ende. 2002). They function as reserve carbohydrates in dicot species such as Jerusalem artichoke (JA; *Helianthus tuberosus*), dahlia (*Dahlia pinnata*), and chicory (*Cichorium intybus*) and are widely used as prebiotics in food, contributing to human and animal health (Roberfroid et al. 2010). Several JA varieties, known to be resilient to many kinds of environmental stresses, are developed for use on saline-alkali soils, counteracting further soil degradation, erosion, and the efficient

✉ Mingxiang Liang
liangmx@njau.edu.cn

1 Jiangsu Key Lab of Marine Biology, College of Resources and Environmental Sciences, Nanjing Agricultural University, Nanjing 210095, Jiangsu, China

2 Institute of Agro-Product Processing, Jiangsu Academy of Agricultural Sciences, Nanjing 210014, Jiangsu, China

3 College of Grassland and Environmental Sciences, Xinjiang Agricultural University, Ürümqi 830052, Xinjiang, China

4 Laboratory of Molecular Plant Biology and KU Leuven Plant Institute, KU Leuven, Kasteelpark Arenberg 31, 3001 Louvain, Belgium

5 Department of Bioengineering, Faculty of Engineering, Marmara University, Istanbul 34722, Turkey

use of land that would otherwise be abandoned (Jiao et al. 2018). Considering its relatively high yields, JA is becoming increasingly popular as feedstock to produce inulin but also bio-fuels and bio-based chemicals in an economically competitive biorefinery (Long et al. 2016). By releasing root exudates, possibly also small inulins, JA is also contributing to an increased diversity and richness of soil microbial communities, preserving and even improving soil quality (Shao et al. 2019). Therefore, growing Jerusalem artichoke on marginal lands and using its inulins can produce fructose from natural origin (hereafter referred to as "bio fructose"). This type of fructose is an easily fermentable feedstock sugar and high fructose syrup which can be biotransformed into value-added products such as single-cell protein and ethanol (Rawat et al. 2017). Although fructose is a more efficient sweetener than sucrose, recent findings do no longer promote its abundant use in food (Helsley et al. 2020). However, fructose serves as a substrate for D-tagatose production (Lee et al. 2017), which is considered a very promising sweetener with important benefits for the treatment of obesity (Guerrero-Wyss et al. 2018).

Microbial fructanases are classified within the glycoside hydrolase family 32 (GH32). Depending on the mechanism employed to hydrolyze fructans, inulinases are classified as either exo-inulinases (E.C.3.8.1.80) or endo-inulinases (E.C.3.2.1.7) (Singh et al. 2017). Endo-inulinases break β-2,1-glycosidic bonds from the internal inulin molecule, yielding reducing type fructooligosaccharides (Fn type FOS), whereas exo-inulinases sequentially cleave terminal fructose units from the nonreducing end of inulin, generating huge amounts of fructose. It is worth noting that some exo-inulinases, levanases, and invertases (also named as non-specific β-fructofuranosidases) have a very broad substrate specificity, being able to hydrolyze inulin, sucrose, or levan (Wanker et al. 1995; Munoz-Gutierrez et al. 2009). Therefore, it is very important to study the substrate specificity of GH32 enzymes in great detail.

In general, microbial inulinases have high industrial value. Inulinases such as those from *Aspergillus* spp., *Penicillium* spp., *Kluyveromyces* spp., (Qiu et al. 2018), and *Alkalibacillus filiformis* (Yousefi-Mokri et al. 2019) have been thoroughly characterized. In this study, we isolated an inulinase-producing bacterial strain, which we identified as *Glutamicibacter mishrai*, from rotten JA tubers. We cloned two exo-inulinase genes from this strain, heterologously expressed the encoded enzymes in *Pichia pastoris*, and characterized their enzymatic properties, providing an explanation for substrate specificity of different INUs based on its structure–function relationship.

Materials and methods

Growth media

The preliminary screenings of inulinase-producing strains were carried out in a medium containing 0.5% NaCl, 0.1% $NH_4H_2PO_4$, 0.1% K_2HPO_4, 0.02% $MgSO_4 \cdot 7H_2O$, and 2% agar (pH 6.8 ± 0.2). One percent inulin (w/v, Sigma, F8052) was added as the only carbon source, selecting for strains that contain high potential inulinase activities. The liquid fermentation medium contained 0.5% NaCl, 0.1% $NH_4H_2PO_4$, 0.1% K_2HPO_4, 0.02% $MgSO_4 \cdot 7H_2O$, 1% inulin, and 0.5% (w/v) peptone.

Isolation, screening, and identification of inulinase-producing strains

Bacterial strains were isolated from rotten Jerusalem artichoke tubers collected from the experimental station at Nanjing Agricultural University, Jiangsu Province. The primary agar plates were incubated at 30 °C for 2–3 days until single colonies appeared, which were then inoculated into 50 mL of liquid fermentation medium (as above) and shaken at 200 rpm at 30 °C for 2–3 days. Bacterial cells were collected by centrifugation at 5,000 × *g* for 5 min at 30 °C and washed in washing buffer (50 mM Tris–HCl, pH 6.0). To induce extracellular inulinase production, the washed cells were transferred into 10 mL of inulinase-producing solution (washing buffer with 1% inulin) and shaken at 200 rpm for 12 h. Supernatant was collected by centrifugation at 5,000 × *g* for 5 min at 4 °C. We incubated a mixture of 0.1 mL of supernatant and 0.9 mL of 50 mM Tris–HCl, pH 6.8 containing 1% inulin at 45 °C in a water bath for 12 h (Jeza et al. 2018; Zhou et al. 2015). The resulting mixture was heated to 95 °C for 5 min to inactivate the enzyme and assayed for reducing sugars using the dinitrosalicylic acid (DNS) method (Miller 1959). Under the same conditions, the supernatant from 0 h inactivated at 95 °C was used as the control and subtracted for enzyme activity analysis. One unit of enzyme was defined as the amount of enzyme needed to produce 1 μmol of reducing sugars per minute from inulin (*I* value, inulinase activity). The *S* value was defined as the amount of enzyme needed to produce 1 micromole of reducing sugars per minute from sucrose (sucrase activity) (Bao et al. 2019). All values were expressed as the average of three independent experiments.

The strain with the highest enzyme production was selected for follow-up studies. The 16S rDNA sequence of the strain was PCR-amplified by primers 27F and 1492R (Table 1) and blasted (http://www.ncbi.nlm.nih.

Table 1 Primers used in this study

Name	Sequence (5′-3′)
27F	**AGAGTTTGATCCTGGCTCAG**
1492R	**GGTTACCTTGTTACGACTT**
Inu1-F	**TTCCCTCTTGCGACAGTCTT**
Inu1-R	**CTGCCTGATCGAGGTGTTCT**
Inu2-F	**GGGAGAAAGTGGTTGTTCCA**
Inu2-R	**TTTCGGGGACTCTTGAATTG**
M13F	**TGTAAAACGACGGCCAGT**
M13R	**CAGGAAACAGCTATGACC**
pic-inu1F	**GGCTGAAGCATCGATGAATTCAATGGCAGCGTTGCCCGA**
pic-inu1R	**GAGATGAGTTTTTGTTCTAGATGCGTTGACCTCCAATGCG**
pic-inu2F	**GGCTGAAGCATCGATGAATTCAGCAGAACTGGGTGATGAACCC**
pic-inu2R	**GAGATGAGTTTTTGTTCTAGAAACTTCGTTGCCGAGGTGAA**
Y1F	**TTTCGATGTTGCTGTTTTGC**
YIR	**GCCCAACTTGAACTGAGGAA**

gov/BLAST/). A 16S rDNA-based phylogenetic tree was constructed using the ClustalV method in the MegAlign program (DNASTAR; Lasergene, v. 7.1).

Medium and process parameter optimization

The strain NJAU-1 colonies were picked and used to inoculate 50 mL of liquid fermentation medium with different carbon source for 24 h to start a seed culture. When the culture reached $OD_{600nm} = 0.6$, 5 mL of seed culture was transferred into 50 mL of fermentation medium (same carbon source as above) and samples were incubated at 30 °C with shaking (200 rpm) for 84 h. The OD_{600nm} of the liquid culture was determined every 12 h and 5 mL supernatant was harvested as above. The effect of various sole carbon sources was investigated (fructose, sucrose, levan, inulin, lactose, glucose, starch, and maltose; 1% w/v). The inulinase activity of the individual supernatants were determined by DNS method as described above. Various trace elements (Ca^{2+}, K^{+}, Na^{+}, Fe^{2+}, Fe^{3+}, Cu^{2+}, Mg^{2+}, Mn^{2+}, Hg^{2+}, Zn^{2}, Co^{2+}, and Li^{+}; 1 mM) were supplemented into 50 mL of fermentation medium to investigate their effect on enzyme production. The effect of fermentation medium pH (5–12, 30 °C) and temperature (10–40 °C; pH 6.0) on inulinase production was also assessed by the DNS method as the above.

Cloning and sequencing of the inu1 and inu2 exo-inulinase genes from Glutamicibacter mishrai NJAU-1

Based on the two candidate *exo-inulinase* gene sequences from the reported S5-52 genome (GenBank: CP032549.1), two primer pairs (Table 1, Inu1F and Inu1R; Inu2F and Inu2R) were designed at the location 200 bp before the upstream open reading frame (ORF) or after the downstream ORF of *inu1* and *inu2* from NJAU-1, respectively. The PCR method was as follows: 95 °C for 3 min; 35 cycles of 95 °C for 15 s, 55 °C for 15 s, and 72 °C for 3 min; and one final extension at 72 °C for 5 min. The resulting PCR products were subcloned into pEASY-Blunt (TransGen) and sequenced by GENEWIZ (Suzhou, China) using M13F and M13R primers (Table 1).

Sequence analysis

The percentage of amino acid sequence similarity among INU1, INU2, and related proteins was determined by BLASTP (http://www.ncbi.nlm.nih.gov/BLAST/). The presence and length of a signal peptide was predicted using SignalP (http://www.cbs.dtu.dk/services/SignalP/). GH32 family members were retrieved from GenBank for sequence alignment analysis using the ClustalV method in the MegAlign program (DNASTAR. Lasergene.v. 7.1). The corresponding phylogenetic tree was then created (CLC Sequence Viewer 6.8).

Production of INU1 and INU2 in Pichia pastoris

INU1 and INU2 proteins were produced in *P. pastoris* strain X33 using the secretory expression vector pPICZαC (EasySelect Pichia Expression Kit, Invitrogen, USA; Wang et al. 2011). The coding sequences without signal peptide were amplified by PCR and digested with *Eco*RI and *Xba*I (TaKaRa) and ligated with pPICZαC vector (pic-inu1F and pic-inu1R; pic-inu2F and pic-inu2R; Table 1) respectively. The resulting constructs were then introduced into *P. pastoris* X33 competent cells (Resina et al. 2004). Positive transformants were identified by PCR analysis using primers Y1F and Y1R (Table 1) and further confirmed by DNA sequencing.

Preparation and purification of crude recombinant inulinase extracts

The whole procedure followed the literature with minor modifications (Xu et al. 2015). 0.5% methanol was added to the medium every 24 h for a total of 5 days, and the OD_{600nm} of the yeast cultures was determined every 12 h and 5 mL supernatant was harvested as above. The activity of crude recombinant inulinase was determined by the DNS method, as described above.

The crude enzyme solution was precipitated with 80% ammonium sulfate and purified by Ni–NTA chelating affinity chromatography with an imidazole gradient of 40, 80, 120, 160, and 200 mM, respectively (Xu et al. 2015). The eluted 6×His-tagged fusion protein was assayed by sodium dodecyl sulfate polyacrylamide gel electrophoresis (SDS-PAGE) using BeyoGel™ Plus Precast PAGE Gel (No. P0505S), following the manufacturer's protocol. The recombinant protein was eluted with imidazole (200 mM) and dialyzed (buffer: 50 mM Tris–HCl, pH 6.8) for 24 h to remove traces of imidazole. The purified INU1 and INU2 proteins were concentrated by ultrafiltration on a Vivaspin 500 Centrifugal Concentrator, with a retention threshold of 30 kDa.

The protein concentration was measured using a TaKaRa Bradford Protein Assay Kit (Code No. T9310A) with bovine serum albumin as standard, following the manufacturer's protocol. Specific activity is defined as the enzyme activity per milligram of protein.

Effects of temperature, pH, metal ions, and substrate on recombinant inulinase activity

To examine the effects of different temperature, the purified recombinant enzymes (100 µL, 0.17 mg/mL) and inulin as substrates (1%, w/v) in 900 µL of 50 mM Tris–HCl, pH 6.8, were incubated from 25 to 60 °C by high-performance liquid chromatography (HPLC) (Xu et al. 2015). To examine the effects of different pH (pH 4.0–6.0: 50 mM sodium acetate; pH 6.0–8.0: Tris–HCl; 30 °C), purified recombinant inulinase activity was determined. To examine the effects of metal ions on recombinant inulinase activity, the assay was performed for 1 h as above with various metal ions at a final concentration of 1 mM. The activity measured in the absence of metal ions was defined as the control. The hydrolysis ability of purified INU1 and INU2 enzymes to substrates (containing different sugars,1% w/v) also was quantified by HPLC, as described (Xu et al. 2015).

Enzyme 3D structure predication and analysis of INU1 and INU2

The homology models of INU1 and INU2 were created through the server https://swissmodel.expasy.org/ (Waterhouse et al. 2018) using *Aspergilus awamori* inulinase (1Y4W) as template. Both homology models were further minimized with a layer of explicit solvent covering 10 Å, and protonated at pH 6.0 using Amber10/14EHT as the force field with a gradient of 0.1 kcal mol^{-1} $A2^{-1}$ in MOE (Molecular Operating Environment, 2019). Sucrose, 1-kestose, nystose, 1^F-fructofuranosylnystose, and inulotriose structures were obtained through the Glycam server (www.glycam.org, accessed: 1 February 2021; Kirschner et al. 2008).

GOLD software was used for the sugar docking analysis (Jones et al. 1997) with ChemPLP as score function. The binding site was defined in the donor nucleophile position (Asp 28 for INU1 and Asp 57 for INU2), selecting all the amino acids flexible in a 20-Å radius. One hundred solutions were generated per analysis, and the complexes with the lowest energies and highest scores were selected for comparison. The interactions were detected and measured by MOE. All figures were prepared using PYMOL 2.4.

Results

Selection of strain Glutamicibacter mishrai NJAU-1

Hundreds of putative inulinase-producing strains were obtained through preliminary screening, after which we determined their enzymatic activity. Among them, four strains had relatively higher enzyme activity (Table 2). The ratio of inulinase over sucrase (I/S) indicated that all strains produced exo-inulinases. The strain *Glutamicibacter mishrai* NJAU-1 (deposited to the China General Microbiological Culture Collection Center, Number: No.19750) exhibited the highest enzymatic activity relative to the other strains, with an *I* value of 0.17 U/mL. Therefore, strain NJAU-1 was selected for deeper studies, further confirming that they harbor genuine exo-inulinases INU1 and INU2 (see below).

We generated a phylogenetic tree based on 16S rDNA sequences from *Glutamicibacter mishrai* NJAU-1 and

Table 2 Enzymatic activity measured in the four isolated strains

Strain	I (U/mL)	S (U/mL)	I/S
A5	0.14 ± 0.001	0.43 ± 0.007	0.33
A7	0.07 ± 0.002	0.89 ± 0.003	0.08
NJAU-1	0.17 ± 0.001	0.85 ± 0.005	0.20
L3	0.03 ± 0.001	0.04 ± 0.001	0.75

Enzyme activity with inulin (Sigma, F8052) as substrate under assay conditions, expressed as *I* value. Enzyme activity with sucrose as substrate under assay conditions, expressed by S value. I/S > 1 is generally considered to be typical for endo-inulinase, while I/S < 1 is generally considered to indicate exo-inulinase activity (Bao et al. 2019). Values represent mean ± SE of three biological replicates

related strains (Fig. 1). NJAU-1 showed the highest similarity with *Glutamicibacter mishrai* S5-52 (99.7%).

Inulinase production peaked at 24 h in Glutamicibacter mishrai NJAU-1

Based on a growth curve analysis (Fig. 2A), we established that *G. mishrai* NJAU-1 reached its maximum biomass after 60 h from a starting OD_{600nm} of 0.4 and then declined thereafter. Maximum inulinase production peaked at 24 h. Within 24 h after inoculation, the strain grew actively and inulinase production increased.

Effect of carbon source

The order of enzyme production induced by various carbon sources was levan > inulin > lactose > glucose > starch. For reference, we set the enzyme production obtained with levan as the sole carbon source to 100%. The enzyme production measured with inulin as sole carbon source reached 46% of levan levels, while lactose, glucose, and starch as sole carbon sources only rose to 15%, 12%, and 13% of levan levels, respectively. We measured no inulinase activity when sucrose, fructose, or maltose was used as the sole carbon source (Fig. 2B).

Effect of different metal ions

The effect of different metal ions on inulinase production varies (Fig. 2C). Enzyme production was highest when 1 mM Ca^{2+} was added to the medium, being 10% higher than the control without metal ion addition. By contrast, the addition of Cu^{2+}, Mn^{2+}, Fe^{3+}, K^{+}, and Fe^{2+} repressed inulinase production, which only accounted for 18%, 67%, 57%, 90%, and 52%, of control production levels without metal ions addition, respectively. The addition of Na^{+} or Li^{+} had little effect on inulinase production, with levels reaching 102% (Na^{+}) and 98% (Li^{+}) of control levels. Notably, the addition of Zn^{2+} or Co^{2+} resulted in no detectable enzyme production.

Effect of temperature and pH

A maximum enzyme production was observed at 15 °C, but production significantly decreased at higher temperatures (Fig. 2D).

We observed an increase in enzyme production with a rise in pH from 5.0 up to a peak at pH 9.0, followed by a decline in production, with a complete loss of enzyme production at pH 12.0 (Fig. 2E). Therefore, we deemed a medium with a pH 8 − 9 to be optimal for enzyme production in the strain. *Glutamicibacter mishrai* NJAU-1 may be successfully grown at low temperatures and high alkalinity to boost inulinase production. Enzyme production (at 15 °C,

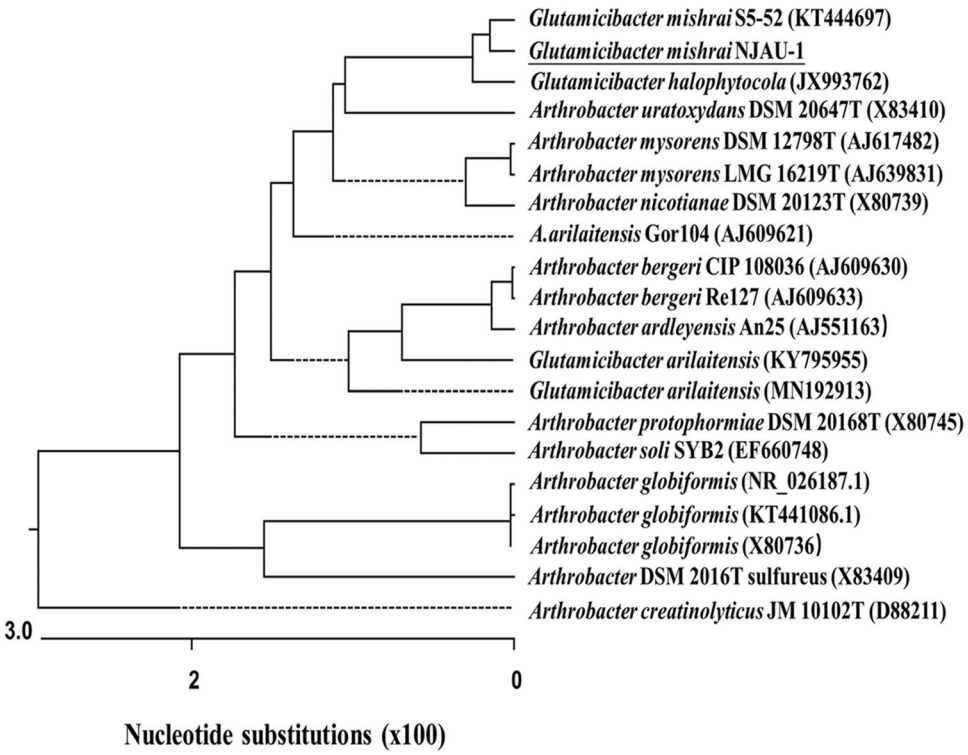

Fig. 1 Phylogenetic tree based on 16S rDNA sequences from *Glutamicibacter mishrai* NJAU-1 and related strains after alignment with ClustalV in the MegAlign program (DNASTAR, Lasergene, v. 7.1). The numbers in parentheses are GenBank IDs. *Glutamicibacter mishrai* NJAU-1 is underlined. The length of each pair of branches represents the distance between sequence pairs. A dotted line on a phenogram indicates a negative branch length, a common result of averaging. Below the tree is a scale indicating the number of "Nucleotide substitutions" per 100 residues for DNA sequences

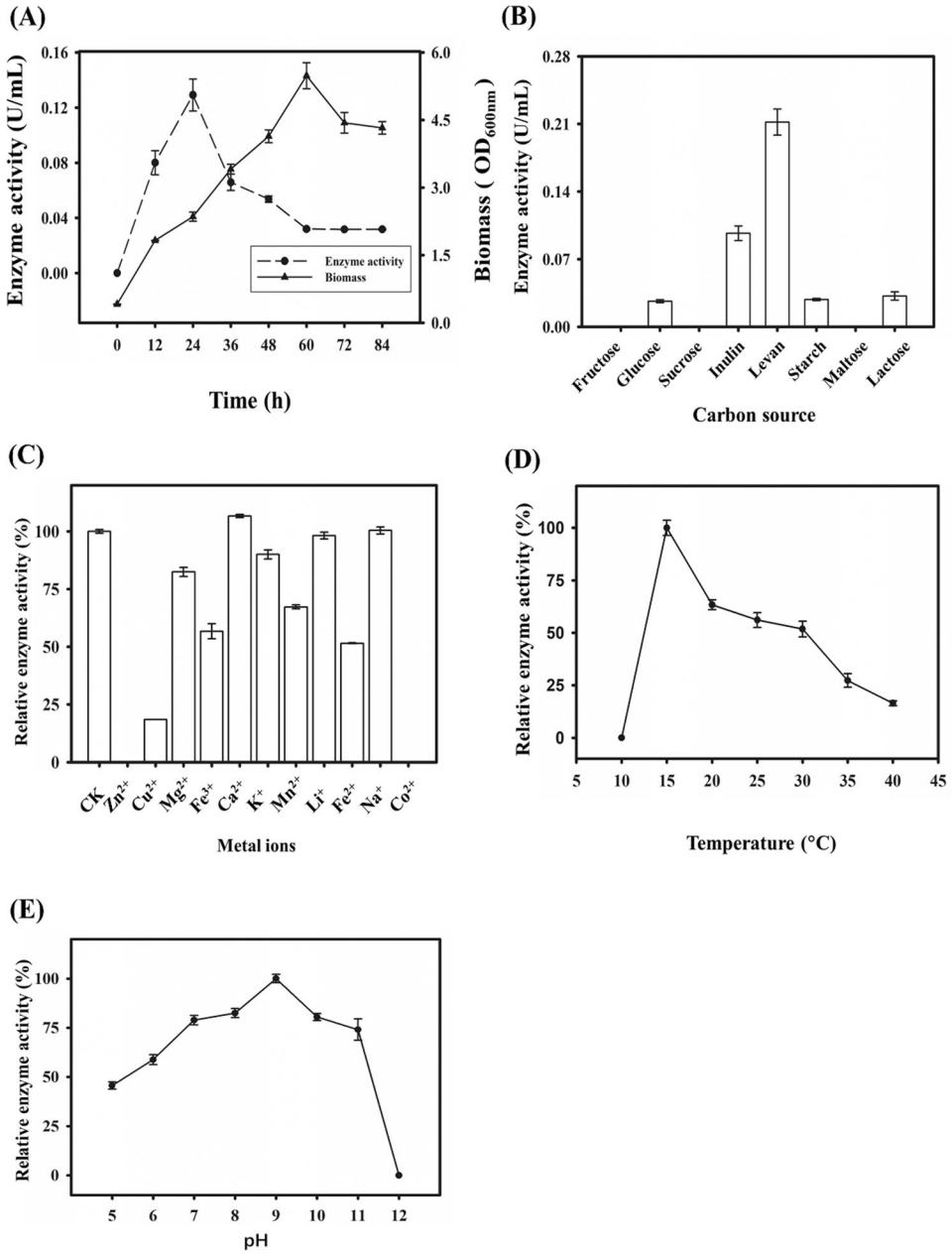

Fig. 2 Effect of growth media on enzyme production. **A** Enzyme production and growth curve of *G. mishrai* NJAU-1 over time. Effect of **B** carbon source, **C** metal ions, **D** pH, and **E** temperature on induce enzyme production. Values represent mean ± SE of three biological replicates

pH 8–9) increased by 90% compared to the original grown parameters (30 °C, pH 6.0).

Two exo-inulinase genes cloned from Glutamicibacter mishrai NJAU-1 showed high similarities with known exo-inulinases

We amplified two putative exo-inulinase genes by PCR from *Glutamicibacter mishrai* NJAU-1 genomic DNA, using the primers Inu1F and Inu1R, and Inu2F and Inu2R (Table 1). The full-length sequence of *inu1* (GenBank: MW355866) was 1482 bp and was predicted to encode a protein of 494 amino acids, whereas that of *inu2* (GenBank: MW355867) was 2616 bp and encoded a predicted protein of 872 amino acids. The predicted putative exo-inulinases both have the conserved motifs NDPNG and FRDP that are common to GH32 family members from different sources (Fig. 3).

INU1 and INU2 shared the highest sequence similarity with the exo-inulinase from *Bacillus subtilis* (GenBank: AAK00768), respectively, reaching 39.6% and 50.2% similarity (Fig. 4). These results suggested that INU1 and INU2 are both exo-inulinases.

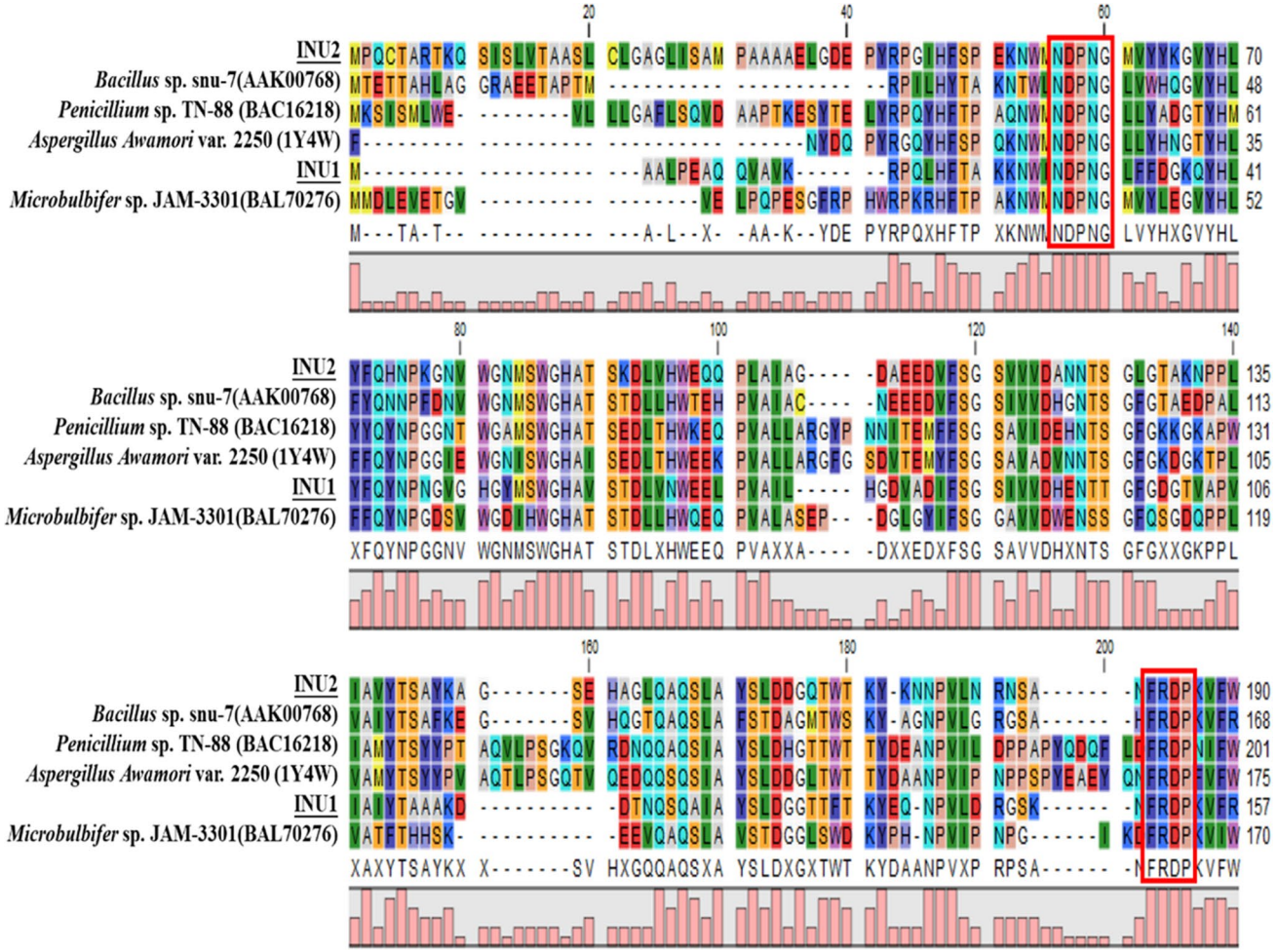

Fig. 3 Amino acid sequence alignment of INU1, INU2, and exo-inulinases from members of glycoside hydrolase (GH) family 32. Sequence names are shown with accession numbers (except INU1 and INU2) as follows: exo-inulinases from *Aspergillus Awamori* var. 2250 (1Y4W), *Microbulbifer* sp. JAM-3301 (BAL70276), *Bacillus* sp. snu-7 (AAK00768), and *Penicillium* sp. TN-88 (BAC16218). The red boxes indicate the NDPNG and FRDP conserved motifs. The pink bar represents the levels of similarity between the six sequences

Expression, purification, and identification of INU1 and INU2

We subcloned INU1 and INU2 coding sequences into a *P. pastoris* expression vector for secretion into the growth medium. A signal peptide search revealed that INU1 has no clear signal peptide (may be intracellular), while INU2 has a signal peptide with a cleavage site between amino acids 34 and 35. The crude enzyme mixture obtained from the supernatant of INU1 cultures exhibited an inulinase activity of 0.85 U/mL after 36 h of incubation. Longer culture times reduced the extractable enzymatic activity (Fig. 5A). The enzymatic activity obtained for INU2 peaked after 24 h of culture and then decreased slightly before stabilizing (6.15 U/mL) (Fig. 5A). Thus, the highest activity from the INU2 crude enzyme preparation was obtained after 24 h of culture and was used for follow-up experiments.

In an SDS-PAGE analysis, purified INU1 migrated as a single band with a molecular mass of approximately 59.0 kDa, which is close to its predicted molecular weight (including the length of the 6×His tag) of 57.2 kDa. The predicted molecular weight of INU2 (without the signal sequence) was about 93.5 kDa, which matched the observed molecular weight (Fig. 5B), confirming that the purified enzymes were INU1 and INU2. INU1 and INU2 were eluted with 200 mM imidazole for further dialysis and ultrafiltration.

Effects of temperature, pH, and metal ions on INU1 and INU2 enzymatic activity from Glutamicibacter mishrai NJAU-1

INU1 specific activity was measured highest at 30 °C and pH 6.0 (0.45 U/mg), while INU2 specific activity peaked

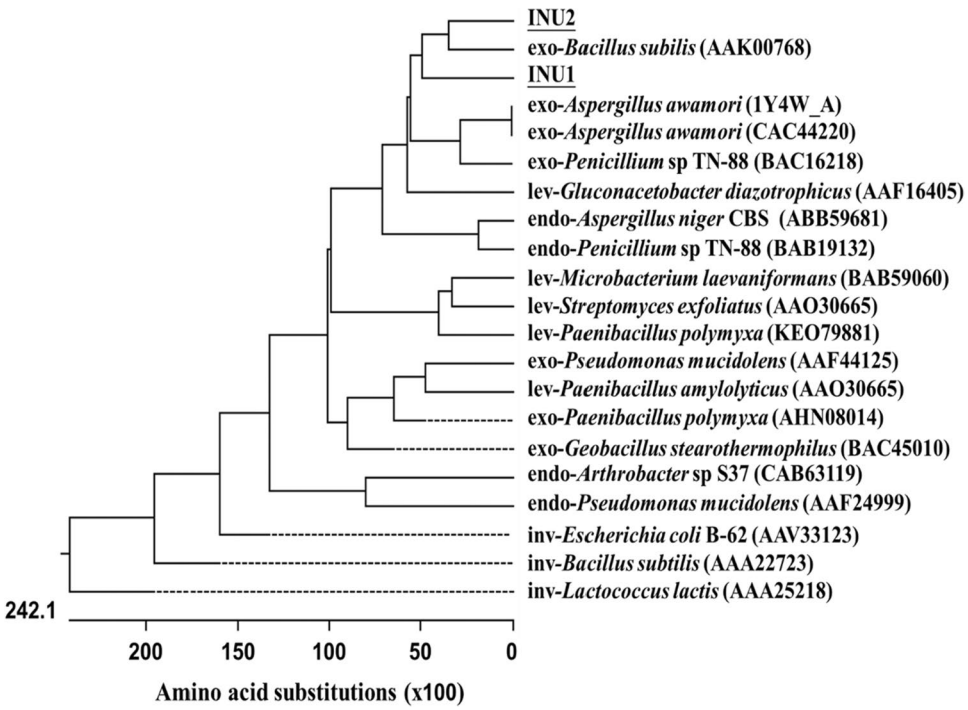

Fig. 4 Phylogenetic tree of INU1 and INU2 based on amino acid sequence analysis with ClustalV in the MegAlign program (DNASTAR. Lasergene. v. 7.1). The numbers in brackets indicate the GenBank IDs (exo-: exo-inulinase; endo-: endo-inulinase; inv-: invertase; lev-: levanase). INU1 and INU2 is underlined. The length of each pair of branches represents the distance between sequence pairs. A dotted line on a phenogram indicates a negative branch length, a common result of averaging. Below the tree is a scale indicating the number of "Amino acid substitutions" per 100 residues for protein sequences

when assayed at 45 °C and pH 6.0 (46.3 U/mg), indicating a different temperature response between the two enzymes (Fig. 5C). Although INU1 and INU2 showed a similar pH optimum (pH 6.0), a different shape of the curve in the acidic region was observed (Fig. 5D), while a strong inhibition was observed under alkaline conditions for both enzymes.

We then tested the effect of ion addition on enzymatic activity. Mg^{2+}, K^{+}, Na^{+}, and Ca^{2+} slightly promoted INU1 activity. The highest INU1 activity was observed with the addition of 1 mM Mg^{2+}, which resulted in a 10% increase in activity over the control without metal ion addition. Mn^{2+}, Fe^{2+}, and Zn^{2+} inhibited INU1 activity and caused a decrease of 12%, 75%, and 80%, respectively, relative to control activity without the addition of metal ions. Cu^{2+} and Fe^{3+} completely blocked INU1 enzymatic activity (Fig. 5E).

Several metal ions promoted INU2 activity, namely (in order of strongest to weakest effect) $Li^{+} > Na^{+} > Co^{2+} > Ca^{2+} > K^{+} > Mg^{2+} > Mn^{2+}$. INU2 activity was highest in the presence of 1 mM Li^{2+}, which increased activity by 20% over control levels without metal ions added (Fig. 5E). Fe^{2+}, Zn^{2+}, Cu^{2+}, and Fe^{3+} inhibited INU2 activity by 20%, 19%, 85%, and 86%, respectively, relative to the control without metal ion addition.

The ability of INU1 and INU2 to hydrolyze different substrates

We established that the ability of purified INU1 to hydrolyze different substrates varied as follows (from the best to the worst): 1-kestose > sucrose > nystose > levan > 1^{F}-fructofuranosylnystose > inulin (Fig. 5F). The ability to hydrolyze 1-kestose was set to 100%. INU1 hydrolyzed sucrose, nystose, levan, and 1^{F}-fructofuranosylnystose to about 68%, 37%, 32%, and 26% of 1-kestose levels, respectively. The ability to hydrolyze inulin was the lowest, at only about 8% of 1-kestose levels. By contrast, purified INU2 showed its highest hydrolysis levels with inulin as its substrate, which was set to 100%. The ability of purified INU2 to hydrolyze 1^{F}-fructofuranosylnystose, nystose, levan, and sucrose was about 99%, 96%, 94%, and 72% of inulin hydrolysis levels, respectively. The ability to hydrolyze 1-kestose was the lowest, at only about 68% (Fig. 5F).

HPLC analysis further revealed that fructose was the primary and also initial hydrolysis product released from inulin by purified INU1 and INU2 (Fig. 6), with relative efficiencies similar to those observed earlier (Fig. 5F). Neither INU1 nor INU2 produced any Fn-type FOS clearly showing that they have no endo-inulinase activity (Fig. 6). INU1 shows a strong hydrolytic activity when incubated with short-chain inulin molecules, while INU2 has a preference for long-chain inulin (Fig. 5F).

3D structure analysis of INU1 and INU2 and sugar docking

In order to better understand the subtle difference in substrate specificity between INU1 and INU2, a molecular docking analysis with various small inulin-type fructans and sucrose was carried out (Fig. 7). For this purpose, 5

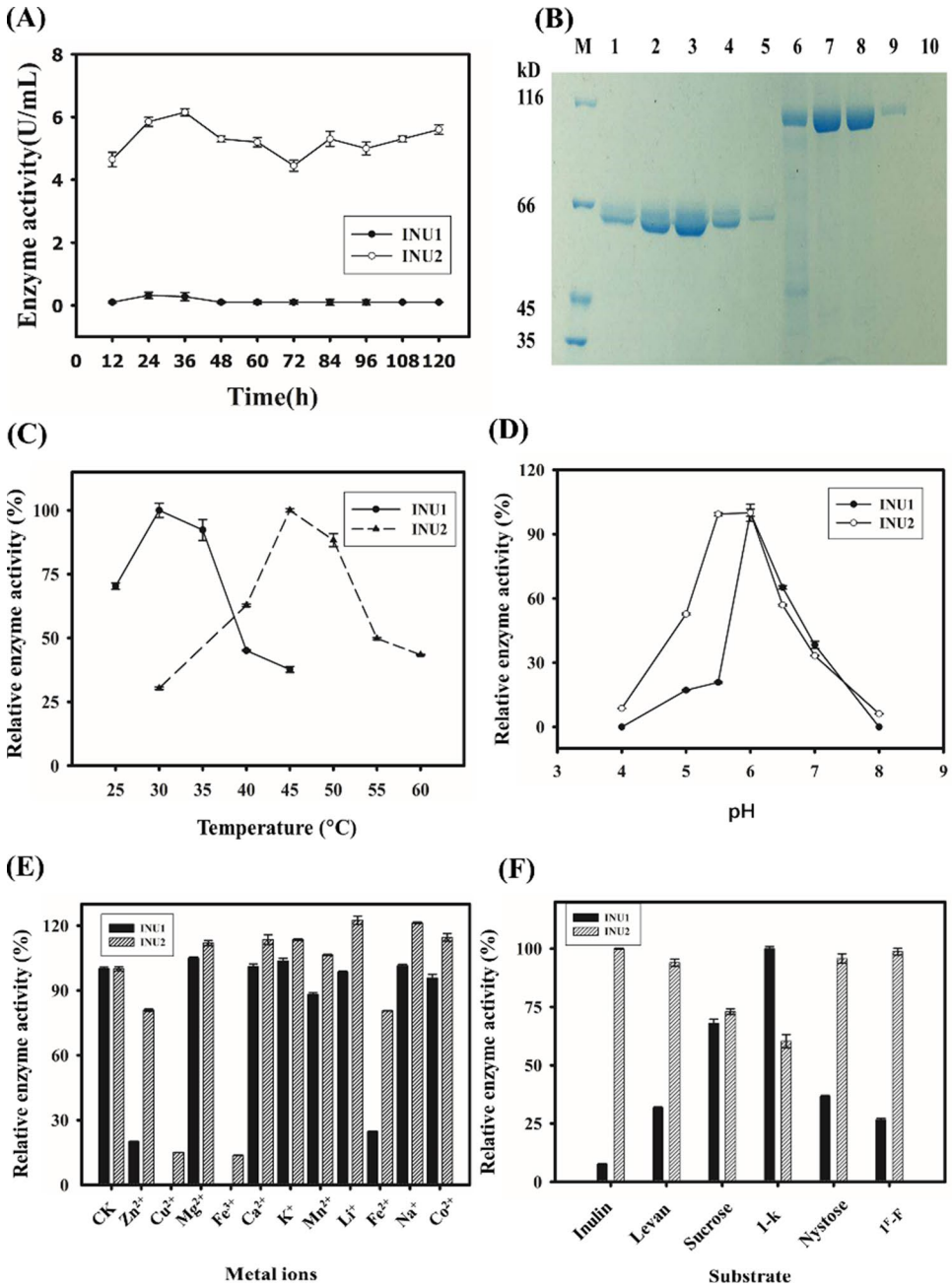

Fig. 5 Enzymatic activity of INU1 and INU2 over time and characterization. **A** Enzymatic activity of INU1 and INU2 produced in *Pichia pastoris*. **B** SDS-PAGE analysis of the recombinant exo-inulinases. M: Marker. Lanes 1–5, INU1 purified by Ni–NTA chelating affinity chromatography with an imidazole gradient of 40, 80, 120, 160, and 200 mM, respectively. Lanes 6–10, INU2 purified by Ni–NTA chelating affinity chromatography with imidazole gradient of 40, 80, 120, 160, and 200 mM, respectively. Effect of **C** temperature (at pH 6.8 assayed), **D** pH (at 30 °C assayed), **E** metal ions, and **F** substrate on inulinase enzymatic activity. Values represent mean ± SE of three biological replicates. 1-K: 1-kestose; 1^F-F: 1F-fructofuranosylnystose

different substrates were docked to the active site regions of both INU1 and INU2. All the terminal fructosyl residues fitted in a catalytical conformation in the − 1 subsite, again confirming the exo-nature of these enzymes (since endo-enzymes show additional − 2, − 3, …subsites). The Fru residue at the − 1 subsite is strongly stabilized by the transition state stabilizer Asp 152 in INU1 and Asp 185 in INU2. In line with the wet work data for sucrose (Fig. 5F), there was no difference in the energy levels of sucrose binding between INU1 and INU2. However, for 1-kestose, the end standing glucose ending is mainly stabilized by His 52 in INU1 but by Trp 81 in INU2 (Fig. 7). As a result of this important difference, a lower energy value was observed for 1-kestose binding to INU1 where His 52 binds in a stronger way through a stacking interaction with the glucose ring. This explains why 1-kestose is the preferential donor substrate for INU1 (Fig. 5F). Structurally, the active site of INU1 showed a high specificity of the subsites − 1, + 1, and + 2. In other words, this enzyme preferentially hydrolyzes the shortest substrates (DP2 and DP3). The reverse is observed for the INU2 enzymes which showed an increasing specificity for nystose and 1^F-fructofuranosylnystose (Fig. 7), where Asn 265, Asp 667, and Asn 670 create strong binding points for the Fru residues residing at the + 3 and + 4 subsites of INU2,

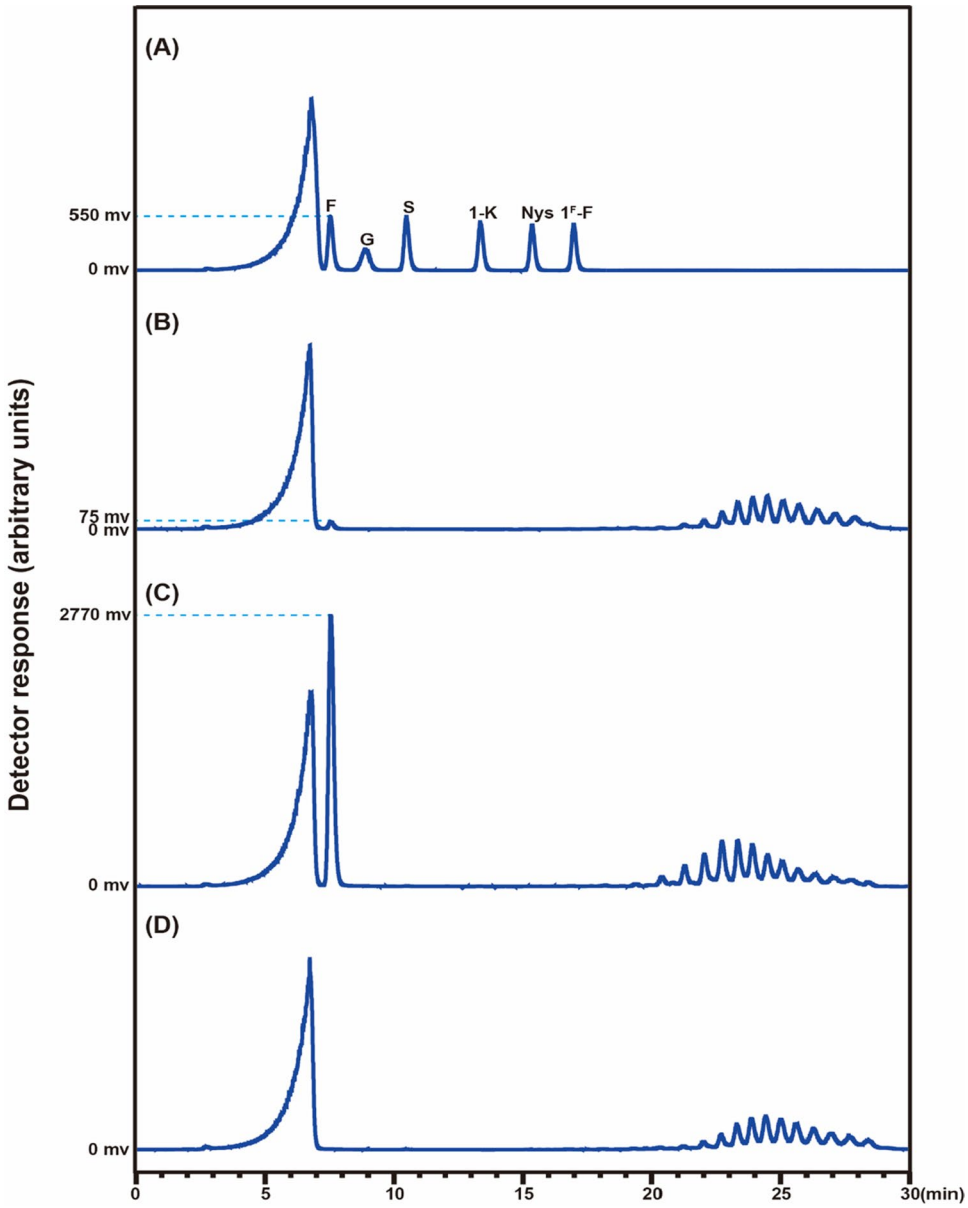

Fig. 6 HPLC analysis of hydrolyzed inulin. (**A**) Mixed standards of fructose (F), glucose (G), sucrose (S), 1-kestose (1-K), nystose (Nys), and 1F-fructofuranosylnystose (1^F-F). (**B**) Hydrolysis products by purified INU1. (**C**) Hydrolysis products by purified INU2. (**D**) Blank control

while these interactions are not observed in INU1. Once again, this in silico result is in perfect agreement with the experimental data (Fig. 5F).

Discussion

Microorganisms with inulinase activity can be isolated from the rhizosphere of inulin-containing plants and naturally decaying inulin-rich material. Most inulinase-producing microorganisms need inulin for induction, while the presence of simple sugars inhibits inulinase production (Beluche et al. 1980; Vandamme and Derycke. 1983). A ratio of inulinase to sucrase activity (I/S) ratio greater than 10^{-2} indicates inulinase activity, while a ratio lesser than 10^{-4} indicates invertase activity (Singh et al. 2017; Vijayaraghavan et al. 2009). I/S > 1 is generally considered to be typical for endo-inulinase, while I/S < 1 is generally considered to indicate exo-inulinase activity (Bao et al. 2019). I/S for all four strains was < 1, indicating that all strains produced exo-inulinases. Colonies growing on medium containing inulin as the sole carbon source may be considered to produce inulinase to sustain their growth (Kango and Jain 2011). In this context, we found a new inulinase-producing strain NJAU-1. No inulinase enzyme was reported from strain S5-52, a *Glutamicibacter mishrae* strain with high similarity with NJAU-1. However, one inulinase was reported from *Arthrobacter* sp. MN8 (Zhou et al. 2015). Recently, the *Arthrobacter* genus was reclassified according to 16S rRNA sequence phylogeny and chemical taxonomic

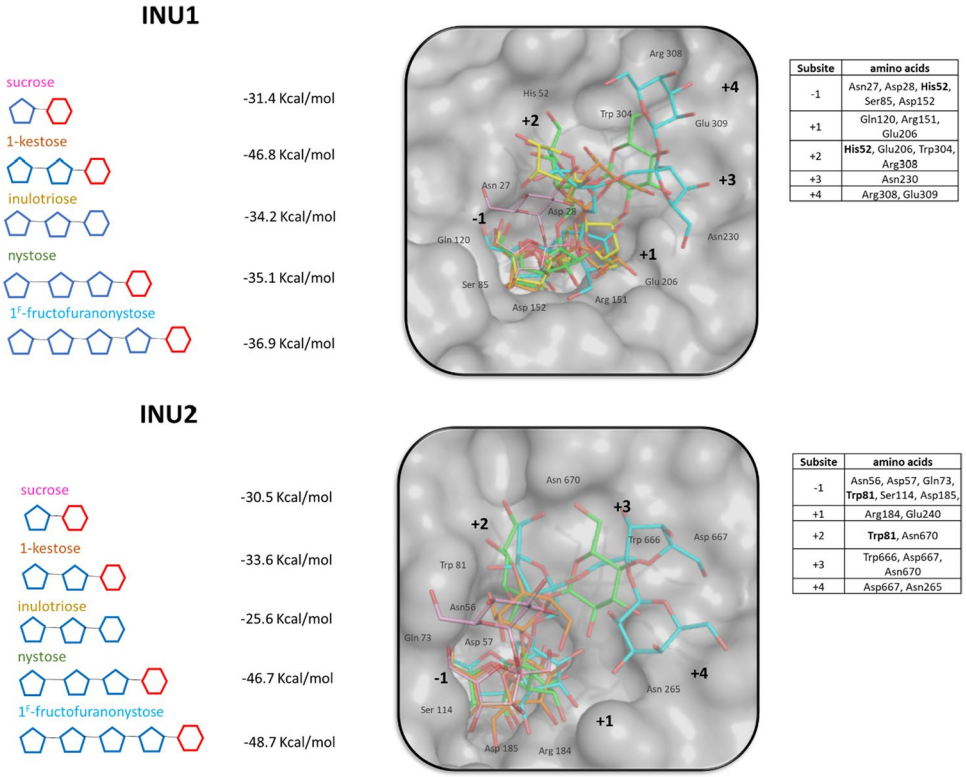

Fig. 7 Binding modes and subsites of INU1 and INU2, determinated by molecular docking with GOLD. The ligands showed are sucrose (pink), 1-kestose (orange), nystose (green), inulotriose (yellow), and 1^F-fructofuranosylnystose (blue). The left side of the figures show the enery values for each substrate (blue residues represent fructose units and red hexagons represent glucose units). The lower the energy values, the stronger the binding. The tables at the right side show the interacting amino acids involved for each subsite. The differential residues His 52 (INU1) and Trp 81 (INU2) are in bold because of their prominent role in substrate specificity

characteristics, and five new genera names were proposed: *Glutamicibacter* gen. nov., *Pseudoglutamicibacter* gen. nov., *Paenarthrobacter* gen. nov., *Paeniglutamicibacter* gen. nov., and *Pseudarthrobacter* gen. nov (Busse, 2016). NJAU-1 is classified under the genus *Glutamicibacter*. Many fungal microorganisms produce inulinase, such as *Aspergillus* sp., *Kluyveromyces* spp., and *Penicillium* spp. (Qiu et al. 2018). *Glutamicibacter mishrai* strain NJAU-1 can now be added to the list of bacteria with inulinase activity, which includes *Arthrobacter* sp. MN8 (Zhou et al. 2015), *Paenibacillus polymyxa* ZJ-9 (Gao et al. 2014), and *Bacillus amyloliquefaciens* NB (Qiu et al. 2019).

In order to improve the production of exo-inulinase during microbial enzyme production, a series of fermentation conditions were optimized. For example, through optimization, *Nocardiopsis* sp. DN-K15 produced 25.1 U/mL of inulinase at pH 9.0 and 37 °C for 60 h, which was 2.7-fold higher than the level in the basal medium (Lu et al. 2014), while the enzyme production of *Kluyveromyces marxianus* YS-1 was increased from 24.7 to 30.8 IU/mL at pH 6.5 and 30 °C for 72 h (Singh et al. 2007).The fermentation time (24 h) for *G. mishrai* NJAU-1 was shorter than the 72 h reported for *Bacillus polymyxa* (Zherebtsov et al. 2002) or 60 h for *Kluyveromyces marxianus* YS-1 (Singh et al. 2007) and *Nocardiopsis* sp. DN-K15 (Lu et al. 2014). Interestingly, the newly isolated NJAU-1 strain from *Glutamicibacter mishrai* can be induced by both levan and inulin for the production of exo-inulinase. Inulin was reported to induce inulinase production in *Arthrobacter* sp. (Elyachioui et al. 1992). This result is also consistent with that reported in *Streptomyces* GNDU 1 and *Nocardiopsis* sp. DN-K15, for which inulin was found to be the best carbon source for inulinase production (Gill et al. 2003; Lu et al. 2014). Inulinase production can also be induced by bacterial levan in *Glutamicibacter mishrai* NJAU-1, but the significance of this finding remains puzzling. However, one hypothesis may be as follows. Since fructans are derived from sucrose in JA roots, they always occur together. So, sucrose and fructans may exude together from JA roots or may be released together after root wounding. Sucrose is efficiently polymerized into levans by many beneficial bacteria from the rhizosphere (e.g., Bacilli; Versluys et al. 2022), offering one possible explanation for the levan-mediated induction of exo-inulinases in *Glutamicibacter mishrai* NJAU-1. This is an exciting new research avenue.

The growth and metabolism of all microorganisms require trace elements, which may function in enzyme biosynthesis (Singh et al. 2008). All strains have specific metal ion quotas (Zherebtsov et al. 2002). The production of inulinase in *Kluyveromyces marxianus* YS-1 was improved by supplementing the growth medium with Mn^{2+} or Ca^{2+}, but it was inhibited by supplementing with Fe^{2+} or Ni^{2+} (Singh et al. 2008). Many *Arthrobacter* strains are cold-adapted bacteria, such as *Arthrobacter* sp. MN8 (Zhou et al. 2015) and *Arthrobacter ureafaciens* K2032 (Coker et al. 2003), and grow at temperatures of 0–5 °C. The maximum enzyme

production from *Glutamicibacter mishrai* NJAU-1 was achieved at 15 °C, which was lower than that reported in other strains. For instance, *Nocardiopsis* sp. DN-K15 produces inulinase at 30 °C (Lu et al. 2014), *Arthrobacter* sp. produces inulinase at 37 °C (Elyachioui et al. 1992), *Penicillium* sp. NFCC 2768 produces inulinase at 30 °C (Rawat et al. 2015), and *Kluyveromyces marxianus* YS-1 produces inulinase at 30 °C, while the enzyme production was significantly reduced at higher temperatures (Singh et al. 2007). The empirically determined optimal pH value of 9.0 for NJAU-1 is higher than that reported for other strains. The inulinase yield of *Flavobacterium* LCB4 is the highest at pH 7.5, and the enzyme cannot be produced if the pH is less than 6.5 or higher than 8.5 (Allais et al. 1986). *Kluyveromyces marxianus* YS-1 increased the enzyme yield as the initial pH value of the medium increased to 6.5, and then decreased (Singh et al. 2007). *Arthrobacter* sp. produces inulinase at pH 7 (Elyachioui et al. 1992). In conclusion, *G. mishrai* NJAU-1 shows a combination of pH (9) and T (15 °C) optimum for exo-inulinase production which may better fit for JA's growth environments. pH of saline-alkali soils generally ranges from 8.0 to 10.0 while JA is tolerant to cold stress and can grow well below 20 °C (Shao et al. 2019; Li et al. 2010). This may also offer opportunities for efficient exo-inulinase production under some exceptional conditions, contributing to reduced heating costs (environmental friendly), and avoided product denaturation or changes (Zhou et al. 2015). Inulin could be more easily hydrolyzed under acidic conditions to produce undesirable color and by-products, such as difructose anhydrides. Working in alkaline conditions also reduces the risk of growth of contaminating micro-organisms (Lu et al. 2014).

The inulinase-producing strains *Pseudomonas mucidolens* (Kwon et al. 2000) and *Bacillus polymyxa* MGL21 (pH 7.0, 35 °C) (Kwon et al. 2003) have only one exo-inulinase. Here, we amplified two putative exo-inulinase genes by PCR from *Glutamicibacter mishrai* NJAU-1 genomic DNA. The molecular weight of INU1 is similar to the inulinase from *Paenibacillus* sp. D9 (58.5 kDa), *Pseudomonas mucidolens* (55 kDa), *Bacillus polymyxa* MGL21 (55.5 kDa), *Bacillus* sp.snu-7 (60 kDa), but the optimum pH and temperature of INU1 (pH 6.0, 30 °C) are different to *Paenibacillus* sp. D9 (pH 4.0, 40 °C) (Jeza et al. 2018), *Pseudomonas mucidolens* (pH 6.0, 55 °C) (Kwon et al. 2000), *Bacillus polymyxa* MGL21 (pH 7.0, 35 °C) (Kwon et al. 2003), and *Bacillus* sp.snu-7 (pH 7.0, 50 °C) (Kim et al. 2004). The molecular weight of INU2 is similar to *Arthrobacter* spp. enzyme (95.1 kDa), but their optimum pH are different (INU2: pH 6.0; *Arthrobacter* spp: pH 5.0–5.5) (Shen et al. 2015). Intriguingly, the shape of the pH curves of INU1 and INU2 was clearly different from one another (Fig. 5D), offering differential possibilities in terms of its application. Intriguingly, the addition of metal ions on enzyme activity yielded results distinct from those reported for other inulinases. For instance, inulinase from *Aspergillus fumigatus* is activated by K^+ and Cu^{2+} but inhibited by Fe^{2+} (Gill et al. 2006) while the inulinase from *Cryptococcus aureus* G7a is activated by Ca^{2+}, K^+, Na^+, Fe^{2+}, and Cu^{2+} and inhibited by Mg^{2+} and Hg^{2+} (Sheng et al. 2008); the inulinase from *Paenibacillus polymyxa* ZJ-9 is activated by Zn^{2+}, Fe^{2+}, and Mg^{2+} and inhibited by Co^{2+} and Cu^{2+} (Gao et al. 2014), and the inulinase from *Pseudomonas mucidolens* is almost completely inhibited by Cu^{2+} and Fe^{3+} and no metal ion is found to increase the exoinulinase activity (Kwon et al. 2000). Compared to reported inulinases from some fungus (the specific activities of purified exo-inulinase from *Penicillium* sp. strain TN-88 and *Kluyveromyces cicerisporus* were 743 U/mg (Moriyama et al. 2002) and 88.7 U/mg (Ma et al. 2016), respectively), specific activities of INU1 (0.45 U/mg) or INU2 (46.3 U/mg) were a little low. Glycosylation of *P. pastoris* X33 expression system may affect INU1 or INU2 enzyme activity (Radoman et al. 2021). The specific activity of purified exo-inulinase (expression in *Escherichia coli*) from *Paenibacillus polymyxa* ZJ-9 was 18.5 U/mg (determined at pH 6.0 and 25 °C, Gao et al. 2014). The specific activity of InuAMN8 (expression in *E. coli*) from *Arthrobacter* sp. MN8 was 62.1 U/mg (determined at pH 7.0 and 35 °C, Zhou et al. 2015).

We demonstrated that INU1 and INU2 are exo-inulinases by a combination of wet work and dry work approaches. Most importantly, we have clearly demonstrated that while INU1 and INU2 have a similar affinity for sucrose, they are clearly different in their preference towards DP3-5 inulin-type FOS. While the affinity of INU1 decreases from DP3 to DP5, the opposite pattern is observed for INU2, which shows the highest affinity for higher DP inulin. Both of two exoinulinases from *Chrysosporium pannorum* shows higher hydrolysis ability to lower DP inulin (Xiao et al. 1989). The docking analysis revealed some important mechanistic insights in the differential functioning of the INU1 and INU2 active sites, in line with the experimental data. The high specificity of INU1 for 1-kestose could be completely attributed to the presence of the His 52 residue in INU1, strongly stabilizing the glucose moiety at the + 2 subsite. Moreover, our preliminary analysis also suggested that His 52 also may play a key role in the pH activity profile (Fig. 5D), being clearly different between INU1 and INU2. Indeed, histidine is a residue that depends on the protonated state to interact in different ways. When it is protonated at low pH, it can interact as an ion. On the other hand, an unprotonated histidine can interact through a stacking with the sugar ring and via H bonds. Knowing that INU1 His 52 is the equivalent residue of Trp 81 in INU2, both are essential for substrate stabilization. However, Trp 81 interactions are not dependent of a pKa equilibrium like it is the case for His 52 in INU1, most probably explaining the differences of pH activity profiles

with a much sharper decrease in relative activity for INU1, when the pH drops from 6.0 to 5.0 (Fig. 5D). On the other hand, Trp 81 also modifies the shape of catalytic site, orienting the longer chain substrates in a different way (Fig. 7), as it is observed for nystose and 1^F-fructofuranosylnystose, reaching strong binding points with Asp 667, Asn 265, and Asn 670, creating the + 3 and + 4 subsites. Probably a similar mechanism may be in place for the longer chain substrates, such as inulin and levan. This hypothesis can be further validated by future side-directed mutagenesis work, modifying the His residue in INU1 into a Trp and/or changing the Trp residue in INU2 into a His. In conclusion, considering signal peptide, different temperature optima, pH curve, and substrate specificity, these two enzymes might act on different environmental conditions.

Acknowledgements We thank Plant editors for valuable comments regarding the manuscript text. This research was supported by grants from the National Key Research and Development Program of China (2020YFD0900704), the Guidance Foundation from the Sanya Institute of Nanjing Agricultural University (NAUSY-MS16), Foreign Experts Project (X202006), Six Talent Peaks Project in Jiangsu Province (SWYY-058), and the Priority Academic Program Development of Jiangsu Higher Education Institutions (PAPD program, 809001). The authors acknowledge Arnout Voet (Laboratory of Biomolecular Modelling and Design, KU Leuven, Belgium) for providing access to GOLD and MOE software. The authors acknowledge FWO Vlaanderen for the financial support.

Author contribution Liang MX: conceptualization, supervision and project administration. Lian D, Zhuang S, Shui C, Zheng SC: investigation. Lian D: methodology and writing—original draft preparation. Ma YH, Sun ZJ, Toksoy Öner E, Van den Ende W: resources, writing—reviewing and editing. Jaime R. Porras-Domínguez: modeling and docking.

Data availability All relevant data are within the manuscript.

Code availability Not applicable.

Declarations

Ethics approval This article does not contain any studies with human participants or animals performed by any of the authors.

Conflict of interest The authors declare no competing interests.

References

Allais JJ, Kammoun S, Blanc F, Girard C, Baratti JC (1986) Isolation and characterization of bacterial strains with inulinase activity. Appl Environ Microbiol 52(5):1086–1090

Bao M, Niu CT, Xu X, Zheng FY, Liu CF, Wang JJ, Li Q (2019) Identification, soluble expression, and characterization of a novel endo-inulinase from *Lipomyces starkeyi* NRRL Y-11557. Int J Biol Macromol 137:537–544

Beluche I, Guiraud JP, Galzy P (1980) Inulinase Activity of *Debaromyces cantarellii*. Folia Microblol 25:32–39

Busse HJ (2016) Review of the taxonomy of the genus *Arthrobacter*, emendation of the genus *Arthrobacter sensu lato*, proposal to reclassify selected species of the genus *Arthrobacter* in the novel genera *Glutamicibacter* gen. nov., *Paeniglutamicibacter* gen. nov., *Pseudoglutamicibacter* gen. nov., *Paenarthrobacter* gen. nov. and *Pseudarthrobacter* gen. nov., and emended description of *Arthrobacter* roseus. Int J Syst Evol Microbiol 66(1):9–37

Coker JA, Sheridan PP, Loveland-Curtze J, Gutshall KR, Auman AJ, Brenchley JE (2003) Biochemical characterization of a β-galactosidase with a low temperature optimum obtained from an antarctic *Arthrobacter* isolate. J Bacteriol 185(18):5473–5482

Elyachioui M, Hornez JP, Tailliez R (1992) General properties of extracellular bacterial inulinase. J Appl Microbiol 73(6):514–519

Gao J, Xu YY, Yang HM, Xu H, Xue F, Li S, Feng XH (2014) Gene cloning, expression, and characterization of an exo-inulinase from *Paenibacillus polymyxa* ZJ-9. Appl Biochem Biotechnol 173(6):1419–1430

Gill PK, Sharma AD, Harchand RK, Singh P (2003) Effect of media supplements and culture conditions on inulinase production by an actinomycete strain. Bioresour Technol 87(2003):359–362

Gill PK, Manhas RK, Singh P (2006) Purification and properties of a heat-stable exoinulinase isoform from *Aspergillus fumigatus*. Bioresour Technol 97(7):894–902

Guerrero-Wyss M, Duran Aguero S, Angarita Davila L (2018) D-tagatose is a promising sweetener to control glycaemia: a new functional food. Biomed Res Int 2018:8718053

Helsley RN, Moreau F, Gupta MK, Radulescu A, DeBosch B, Softic S (2020) Tissue-specific fructose metabolism in obesity and diabetes. Curr Diab Rep 20(11):64

Jeza S, Maseko SB, Lin J (2018) Purification and characterization of exo-inulinase from Paenibacillus sp. d9 strain. Protein J 37(1):70–81

Jiao J, Wang J, Zhou MJ, Ren XY, Zhan WY, Sun ZJ, Zhao HY, Yang Y, Liang MX, Van den Ende W (2018) Characterization of fructan metabolism during Jerusalem artichoke (Helianthus tuberosus L.) germination. Front Plant Sci 9:1384

Jones G, Willett P, Glen RC, Leach AR, Taylor R (1997) Development and validation of a genetic algorithm for flexible docking. J Mol Biol 267:727–748

Kango N, Jain SC (2011) Production and properties of microbial inulinases: recent advances. Food Biotechnol 25(3):165–212

Kim KY, Koo BS, Jo D, Kim SI (2004) Cloning, expression, and purification of exoinulinase from Bacillus sp. snu-7. J Microbiol Biotechn 14(2):344–349

Kirschner KN, Yongye AB, Tschampel SM, González-Outeiriño J, Daniels CR, Foley L, Woods RJ (2008) GLYCAM06: a generalizable biomolecular force field. Carbohydrates. J Comput Chem 29(4):622–655

Kwon YW, Kim HY, Choi YJ (2000) Cloning and characterization of *Pseudomonas mucidolens* exoinulinase. J Microbiol Biotechn 10(2):238–243

Kwon HJ, Jeon SJ, You DJ, Kim KH, Jeong YK, Kim YH, Kim YM, Kim BW (2003) Cloning and characterization of an exoinulinase from *Bacillus polymyxa*. Biotechnol Lett 25(2):155–159

Lee SH, Hong SH, Kim KR, Oh DK (2017) High-yield production of pure tagatose from fructose by a three-step enzymatic cascade reaction. Biotechnol Lett 39(8):1141–1148

Li XF, Hou SL, Su M, Yang MF, Shen SH, Jiang GM, Qi DM, Chen SY, Liu GS (2010) Major energy plants and their potential for bioenergy development in China. Environ Manage 46(4):579–589

Long XH, Shao HB, Liu L, Liu LP, Liu ZP (2016) *Jerusalem artichoke*: a sustainable biomass feedstock for biorefinery. Renew Sust Energ Rev 54:1382–1388

Lu WD, Li AX, Guo QL (2014) Production of novel alkalitolerant and thermostable inulinase from marine actinomycete Nocardiopsis

sp. DN-K15 and inulin hydrolysis by the enzyme. Ann Microbiol 64(2):441–449
Ma JY, Cao HL, Tan HD, Hu XJ, Liu WJ, Du YG, Yin H (2016) Cloning, expression, characterization, and mutagenesis of a thermostable exoinulinase from *Kluyveromyces cicerisporus*. Appl Biochem Biotechnol 178(1):144–158
Miller GL (1959) Use of dinitrosalicyclic acid reagent for determination of reducing sugar. Anal Chem 31:426–428
Moriyama S, Akimoto H, Suetsugu N, Kawasaki S, Nakamura T, Ohta K (2002) Purification and properties of an extracellular exoinulinase from Penicillium sp strain TN-88 and sequence analysis of the encoding gene. Biosci Biotechnol Biochem 66(9):1887–1896
Munoz-Gutierrez I, Rodriguez-Alegria ME, Munguia AL (2009) Kinetic behaviour and specificity of beta-fructosidases in the hydrolysis of plant and microbial fructans. Process Biochem 44(8):891–898
Qiu YB, Lei P, Zhang YT, Sha YY, Zhan YJ, Xu ZQ, Li S, Xu H, Ouyang PK (2018) Recent advances in bio-based multi-products of agricultural *Jerusalem artichoke* resources. Biotechnol Biofuels 11:151
Qiu YB, Zhu YF, Zhan YJ, Zhang YT, Sha YY, Zhan YJ, Xu ZQ, Li S, Feng XH, Xu H (2019) Systematic unravelling of the inulin hydrolase from *Bacillus amyloliquefaciens* for efficient conversion of inulin to poly-(γ-glutamic acid). Biotechnol Biofuels 12:145
Radoman B, Grunwald-Gruber C, Schmelzer B, Zavec D, Gasser B, Altmann F, Mattanovich D (2021) The degree and length of o-glycosylation of recombinant proteins produced in *Pichia pastoris* depends on the nature of the protein and the process type. Biotechnol J 16(3):e2000266
Rawat HK, Jain SC, Kango N (2015) Production and properties of inulinase from Penicillium sp. NFCC 2768 grown on inulin-rich vegetal infusions. Biocatal Biotransfor 33(1):61–68
Rawat HK, Soni H, Treichel H, Kango N (2017) Biotechnological potential of microbial inulinases: recent perspective. Crit Rev Food Sci Nutr 57(18):3818–3829
Resina D, Serrano A, Valero F, Ferrer P (2004) Expression of a *Rhizopus oryzae lipase* in *Pichia pastoris* under control of the nitrogen source-regulated formaldehyde dehydrogenase promoter. J Biotechnol 109(1–2):103–113
Roberfroid M, Gibson GR, Hoyles L, McCartney AL, Rastall R, Rowland I, Wolvers D, Watzl B, Szajewska H, Stahl B, Guarner F, Respondek F, Whelan K, Coxam V, Davicco MJ, Leotoing L, Wittrant Y, Delzenne NM, Cani PD, Neyrinck AM, Meheust A (2010) Prebiotic effects: metabolic and health benefits. Br J Nutr 104:S1–S63
Shao TY, Gu XY, Zhu TS, Pan XT, Zhu Y, Long XH, Shao HB, Liu MQ, Rengel Z (2019) Industrial crop *Jerusalem artichoke* restored coastal saline soil quality by reducing salt and increasing diversity of bacterial community. Appl Soil Ecol 138:195–206
Shen JD, Zhang R, Li JJ, Tang XH, Li RX, Wang M, Huang ZX, Zhou JP (2015) Characterization of an exo-inulinase from *Arthrobacter*: a novel NaCl-tolerant exo-inulinase with high molecular mass. Bioengineered 6(2):99–105
Sheng J, Chi ZM, Gong F, Li J (2008) Purification and characterization of extracellular inulinase from a marine yeast *Cryptococcus aureus* G7a and inulin hydrolysis by the purified inulinase. Appl Biochem Biotechnol 144(2):111–121
Singh RS, Bhermi HK (2008) Production of extracellular exoinulinase from *Kluyveromyces marxianus* YS-1 using root tubers of *Asparagus officinalis*. Bioresour Technol 99(15):7418–7423
Singh RS, Sooch BS, Puri M (2007) Optimization of medium and process parameters for the production of inulinase from a newly isolated *Kluyveromyces marxianus* YS-1. Bioresour Technol 98(13):2518–2525
Singh RS, Chauhan K, Kennedy JF (2017) A panorama of bacterial inulinases: production, purification, characterization and industrial applications. Int J Biol Macromol 96:312–322
Van Laere A, Van den Ende W (2002) Inulin metabolism in dicots: Chicory as a model system. Plant Cell Environ 25(6):803–813
Vandamme EJ, Derycke DG (1983) Microbial inulinases: fermentation process, properties, and applications. Adv Appl Microbiol 29:139–176
Versluys M, Porras-Domínguez JR, De Coninck T, Van Damme EJM, Van den Ende W (2022) A novel chicory fructanase can degrade common microbial fructan product profiles and displays positive cooperativity. J Exp Bot 73(5):1602–1622
Vijayaraghavan K, Yamini D, Ambika V, Sravya Sowdamini N (2009) Trends in inulinase production-a review. Crit Rev Biotechnol 29(1):67–77
Wang L, Huang Y, Long X, Meng X, Liu Z (2011) Cloning of exoinulinase gene from *Penicillium janthinellum* strain B01 and its high-level expression in *Pichia pastoris*. J Appl Microbiol 111(6):1371–1380
Wanker E, Huber A, Schwab H (1995) Purification and characterization of the *Bacillus subtilis* levanase produced in *Escherichia coli*. Appl Environ Microbiol 61(5):1953–1958
Waterhouse A, Bertoni M, Bienert S, Studer G, Tauriello G, Gumienny R, Heer FT, de Beer TAP, Rempfer C, Bordoli L, Lepore R, Schwede T (2018) SWISS-MODEL: homology modelling of protein structures and complexes. Nucleic Acids Res 46(W1):W296–W303
Xiao R, Tanida M, Takao S (1989) Purification and characteristics of two exoinulinases from *Chrysosporium pannorum*. J Ferment Bioeng 67(5):331–334
Xu HH, Liang MX, Xu L, Li H, Zhang X, Kang J, Zhao QX, Zhao HY (2015) Cloning and functional characterization of two abiotic stress-responsive *Jerusalem artichoke* (*Helianthus tuberosus*) fructan 1-exohydrolases (1-FEHs). Plant Mol Biol 87(1–2):81–98
Yousefi-Mokri M, Sharafi A, Rezaei S, Sadeghian-Abadi S, Imanparast S, Mogharabi-Manzari M, Amanzadeh Y, Faramarzi MA (2019) Enzymatic hydrolysis of inulin by an immobilized extremophilic inulinase from the halophile bacterium *Alkalibacillus filiformis*. Carbohydr Res 483:107746
Zherebtsov NA, Shelamova SA, Abramova IN (2002) Biosynthesis of inulinases by *Bacillus* bacteria. Appl Biochem Biotechnol 38(6):634–638
Zhou JP, Lu Q, Peng MZ, Zhang R, Mo MH, Tang XH, Li JJ, Xu B, Ding JM, Huang ZX (2015) Cold-active and NaCl-tolerant exo-inulinase from a cold-adapted Arthrobacter sp MN8 and its potential for use in the production of fructose at low temperatures. J Biosci Bioeng 119(3):267–274